

# Assistance Control Method for One-Leg Pedaling Motion of a Cycling Wheelchair

Aya Kaisumi<sup>1</sup>, Yasuhisa Hirata<sup>1</sup> and Kazuhiro Kosuge<sup>1</sup>

**Abstract**—Since the cycling wheelchair was introduced in the 2000s, we have focused on alleviating the over-use of healthy limbs that presents a problem to users. To this end, we have been developing assistance control for everyday users of cycling wheelchairs. In our previous research, we found that user load varies in different environments. Traveling resistance compensation control proved successful in counteracting in a range of environments. In the user-load investigation on cycling wheelchairs, the crank torque generated by pedaling was observed to be problematic for hemiplegic patients, who must pedal mainly with their healthy side. Furthermore, for patients able to bend one leg only, because the opposite limb is stiffened at the knee joint or physically absent, the cycling wheelchair is difficult to maneuver. This paper focuses on the crank torque during one-leg-pedaling and proposes a new assistance control.

## I. INTRODUCTION

Currently, individuals with lower-limb disabilities can access a range of equipment such as wheelchairs, walkers, and electric mobility devices. Daily use of such equipment may lead to over-use of healthy parts and disuse of disabled parts. For example, wheelchairs are popular mobility tools because they are low-cost and can assist a wide range of patients with lower-limb disabilities. However, persistent use of the upper limbs to roll the wheelchair may eventually hurt the joints. On the other hand, immobility of lower limbs may cause “disuse syndrome” that threatens blood circulation. Furthermore, because they must be rolled by both arms, wheelchairs are not easily maneuverable by hemiplegic patients.

The cycling wheelchair originated from functional electrical stimulation (FES) research [1]. Cycling wheelchair users pedal with both legs. Despite the presumed difficulty of disabled lower-limb patients pedaling with their legs, many patients can successfully do so [2]. Cycling wheelchairs are also beneficial in rehabilitation, since the act of pedaling increases the muscle activity of hemiplegic patients [3].

A top view and mechanical construction of the cycling wheelchair are shown in Fig.1. The front pedals are connected to the right wheel. The direction is controlled by the steering wheel, operated by the hand lever. The cycling wheelchair may be purchased from TESS Co. Ltd., Sendai, Japan.

The cycling wheelchair provides a solution to the disuse syndrome, and has been used to rehabilitate lower-limb paraplegic and hemiplegic patients in indoor facilities. Recently,

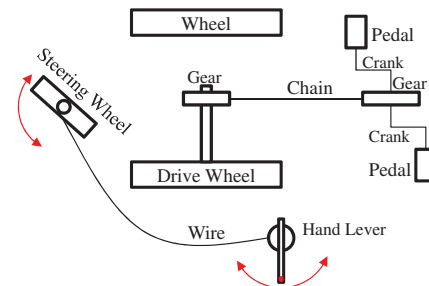


Fig. 1: Top View of Cycling Wheelchair

it is becoming more widely used and has integrated into daily living. Our research aims to retain the exercise benefits while removing the difficulty of cycling wheelchair use, especially for everyday and long-term users, by augmenting the cycling wheelchair with an actuating motor and a few sensors.

Everyday users of the cycling-wheelchair encounter environmental problems as uphill slopes. Our previous research investigated user load in various daily environments, as perceived by lower-limb disabled subjects and healthy control subjects. User load was observed to significantly vary in different environments; in particular, environs that are difficult to negotiate increase the risk of accidents. In addition, we found that hemiplegic patients pedal mainly with their healthy side, thereby applying double force to that side to compensate the disabled side. This asymmetry incurs a risk of over-use of the healthy side [4].

To correct the environmental dependence on user load, we previously equipped the cycling wheelchair with traveling resistance compensation control. Such control successfully canceled the resistance introduced by complex environments. This paper focuses on the latter part of the problem; that of asymmetric pedaling by hemiplegic patients. For patients with a single bendable leg, the cycling wheelchair is especially difficult to maneuver.

We determine the pedaling characteristics by investigating one-leg pedaling. We discuss crank torque during pedaling

<sup>1</sup>Department of Bioengineering and Robotics, Tohoku University  
 6-6-01 Aramaki Aoba, Aoba-ku, Sendai, 980-8579 JAPAN  
 kaisumi@irs.mech.tohoku.ac.jp

and propose a new assistance control for one-leg pedaling.

Section 2 introduces related studies. The basic idea of the proposed control is discussed in Section 3. The pedaling characteristics which are important to develop assistance control for one-leg-pedaling, are discussed in Section 4. Sections 5 and 6 describe and test the assistance control method, respectively.

## II. RELATED STUDIES

The cycling wheelchair, and its daily use, has recently featured in robotics and virtual reality studies. Hirata et al. proposed a regenerative brake control with passive behavior to assist braking a cycling wheelchair, for example when it is on downhill incline, to prevent overspeed [5]. Hiro et al. developed a measurement system for cycling wheelchairs [6] in which environmental data are collected by a variety of mounted sensors and motors. This system alerts the user to pending unrecognized dangers such as obstacles and pedestrians. Navigation and power support is also available for traveling longer distance travel.

Sugita et al. developed a virtual reality system for cycling-wheelchairs [7]. This virtual reality system is necessary because users require large space for mastering the cycling wheelchair before entering everyday life. Driving skill indices of the cycling wheelchair such as pedaling balance, pedaling speed control, and handle steering were evaluated in this system. Moreover, navigation skill was evaluated and compared between young and elderly subjects in a scenario of the virtual reality system [8].

Pedaling studies related to the current work have focused on rehabilitation with functional electric stimulation (FES), rehabilitation with ergometer, robotic pedaling, and power-assisted cycling.

FES pedaling has been thoroughly researched because pedaling is regarded as more efficient at converting muscle force to driving force than other locomotive activities such as walking. Based on a dynamic musculo-skeletal model, Schutte et al. improved FES efficiency by ergometric optimization of seat configurations such as the recline angle of the seat-back, orientation of the seat relative to gravity, and distance between the hip and crank centers [9]. Gföhler et al. developed an optimized stimulation pattern of FES based on a model of electrically stimulated muscle and investigated the correlation between muscle activity and pedaling rate [10]. In addition, they studied an alternative cycling design using a freely-adjustable test bed and assessed the influence of geometry and individual parameters on FES [11]. The above researches have elucidated muscle stimulation patterns, optimal geometric system configurations, and efficiency of FES rehabilitation. Rosecrance et al. analyzed lower-limb movement during ergometer pedaling and compared hemiplegics and nonhemiplegics [12]. Brown et al. revealed that muscle activity adapts to the anti-gravity posture during pedaling, and that increased workload enhances force output by the hemiplegic leg [13], [14]. Saitou et al. studied cerebral blood volume and oxygenation during rehabilitation tasks [15]. These studies focused on the effects of pedaling for

hemiplegic individuals and revealed the pedaling motion used by hemiplegics. However, the rehabilitation workloads used in these studies are constant during pedaling.

In robotics, Nakanishi et al. realized pedaling motions by a self-trained musculo-skeletal humanoid robot [16]. Kosuge et al. proposed load-free power-assistance control for bicycles [17]. This system compensates the drag force imposed by the environment yielding the same riding experience as a horizontal road. As mentioned above, pedaling has been extensively researched. However, previously proposed systems for power assistance control have assumed bipedal action and are not applicable to one-leg pedaling. To realize assistance control for one-leg pedaling, we must characterize the pedaling torque throughout one cycle of one-leg pedaling.

This paper discusses the characteristics of one-leg pedaling obtained by a motor attached to a user-driven cycling wheelchair. A new control algorithm for one-leg pedaling is proposed.

## III. CONCEPT OF THE PROPOSED ASSISTIVE CONTROL METHOD FOR ONE LEG PEDALING

The basic idea of the proposed pedaling assistive control system is to expand the basic power-assisted control considering pedaling characteristics. In conventional power-assisted control, the assistive torque is calculated by multiplying the human torque input with a constant, as follows:

$$\tau_a = Q\tau_{\text{input}}, \quad (1)$$

where  $\tau_{\text{input}}$  is the input torque to the pedal,  $\tau_a$  is the assistive torque, and  $Q$  is the multiplying constant. This type of power-assisted control has been effectively used for bicycles. However, this control is not applicable to hemiplegic pedaling. Because for this control, the input is multiplied by a constant, the uneven pedaling torque pattern is magnified that pedaling with the healthy leg becomes easier and pedaling with the affected leg becomes yet more difficult.

In our proposed method, we set a hypothesis that pedaling input torque consists of human operating torque and gravity effects of legs.

The concepts of our proposed control method are; (a) to assist human operating torque instead of pedaling input torque, and (b) to replace the multiplying constant  $Q$  with a coefficient function of angle of the crank  $\theta$ ,  $R_{\text{assist}}(\theta)$ , as follows:

$$\tau_a = R_{\text{assist}}(\theta)\tau_h \quad (2)$$

In the following sections, first a one-leg model is discussed and the human operating torque  $\tau_h$  is obtained. Next, the specifics of the function  $R_{\text{assist}}(\theta)$  is discussed.

## IV. CHARACTERISTICS OF ONE-LEG PEDALING

This section discusses the characteristics of one-leg pedaling to verify the hypothesis that human pedaling motion consists of operating torque and gravity effect on the leg. The operating torque is exerted by leg joint torques. We define operating torque as  $\tau_h$  and torque by gravity effect on the leg as  $\tau_g$ . The human operating torque and torque by

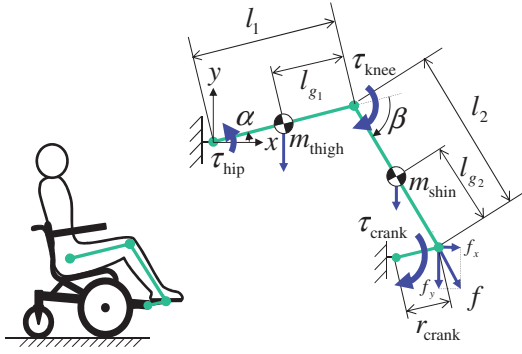


Fig. 2: Model of Human Leg

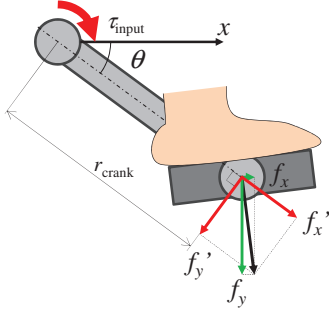


Fig. 3: Definition of Crank Angle  $\theta$

gravity effect are calculated individually and the resulting input torque  $\tau_{input}$  is compared with measured data.

A model of the human leg is shown in Fig.2. The human leg is approximated by a three degrees of freedom (DOF) link mechanism in the 2-dimensional Euclidean plane, assuming freedom of the ankle joint and that pedaling force is mainly applied by the knee and hip joints.

Joint angles  $\alpha$  and  $\beta$  are defined as shown in the figure; i.e.,  $\alpha$  is the angle between thigh and the global  $x$  axis (parallel to the ground) and  $\beta$  is the angle between thigh and shin. The leg tip is subjected to horizontal and vertical force components, denoted  $f_x$  and  $f_y$ , respectively.  $\tau_{hip}$  and  $\tau_{knee}$  are the torques generated by the hip and knee joints, respectively. The length  $l_1$  and  $l_2$  are length of thigh and shin, respectively, where the distance  $l_{g1}$  is the distance between knee and the center of mass of thigh, and  $l_{g2}$  is the distance between ankle and the center of mass of shin. The mass  $m_{thigh}$  and  $m_{shin}$  are the mass of thigh and shin, respectively.

The forces applied to the tip of the leg,  $f_x$  and  $f_y$ , are obtained from the joint torques  $\tau_{hip}$  and  $\tau_{knee}$ .

$$\begin{aligned} \begin{bmatrix} f_x \\ f_y \end{bmatrix} &= (\mathbf{J}^T)^{-1} \begin{bmatrix} \tau_{hip} \\ \tau_{knee} \end{bmatrix} \\ &= \left( \begin{bmatrix} \frac{\partial X_{foot}}{\partial \alpha} & \frac{\partial X_{foot}}{\partial \beta} \\ \frac{\partial Y_{foot}}{\partial \alpha} & \frac{\partial Y_{foot}}{\partial \beta} \end{bmatrix}^T \right)^{-1} \begin{bmatrix} \tau_{hip} \\ \tau_{knee} \end{bmatrix}, \end{aligned} \quad (3)$$

where  $\mathbf{J}$  is the Jacobi matrix containing the leg tip position  $(X_{foot}, Y_{foot})$  and joint angles  $\alpha$  and  $\beta$ .

The forces perpendicular and parallel to the crank,  $f'_x$  and  $f'_y$ , respectively, are obtained from the rotation matrix of the

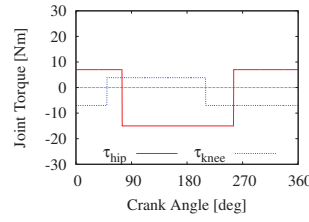


Fig. 4: Input Joint Torque

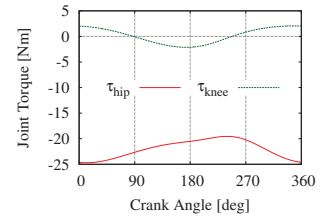
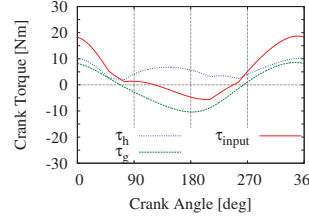
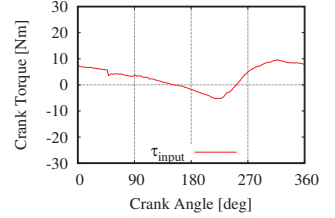


Fig. 5: Gravity on Each Joints



(a) Simulated Pedaling



(b) Measured Pedaling

Fig. 6: Comparison of Simulated and Measured Pedaling

crank angle  $\theta$ , defined in Fig.3, ranges from  $0^\circ$ – $360^\circ$ . Its initial position is when  $\theta = 0$ .

$$\begin{bmatrix} f'_x \\ f'_y \end{bmatrix} = \mathbf{rot}(\theta) \begin{bmatrix} f_x \\ f_y \end{bmatrix}. \quad (4)$$

The operating crank torque  $\tau_h$  is obtained from  $f'_y$  as

$$\tau_h = f'_y r_{crank}. \quad (5)$$

We now introduce the effect of gravity. The crank torque imposed by gravity is

$$\tau_{g_{hip}} = -\frac{\partial X_{thigh}}{\partial \alpha} m_{thigh} g - \frac{\partial X_{shin_h}}{\partial \beta} m_{shin} g, \quad (6)$$

$$\tau_{g_{knee}} = -\frac{\partial X_{shin_k}}{\partial \beta} m_{shin} g, \quad (7)$$

$$\begin{bmatrix} f'_{gx} \\ f'_{gy} \end{bmatrix} = \mathbf{rot}(\theta) \left( \begin{bmatrix} \frac{\partial X_{foot}}{\partial \alpha} & \frac{\partial X_{foot}}{\partial \beta} \\ \frac{\partial Y_{foot}}{\partial \alpha} & \frac{\partial Y_{foot}}{\partial \beta} \end{bmatrix}^T \right)^{-1} \begin{bmatrix} \tau_{g_{hip}} \\ \tau_{g_{knee}} \end{bmatrix}, \quad (8)$$

$$\tau_g = (f'_{gx} - f'_{gy}) r_{crank}, \quad (9)$$

where  $(X_{thigh}, Y_{thigh})$  and  $(X_{shin}, Y_{shin})$  are the positions of the center of gravity of thigh and shin, respectively, and  $g$  is gravitational acceleration.

The net pedaling torque is the sum of the individual torque:

$$\tau_{input} = \tau_h + \tau_g \quad (10)$$

Leg joint torques  $\tau_{hip}$  and  $\tau_{knee}$  are given as shown in Fig.4 to simulate the pedaling torque. The given joint torques are decided so that they follow potential human leg joint torques, referring to studies by Samuel et al, Bento et al. and Pontaga [18]–[20].

The driving torque calculated from the above torque is plotted as a function of crank angle in Fig.6. For comparison the measured driving torque is plotted in Fig.6. These

TABLE I: Torque Exertion Ranges of Healthy Human Leg

Gender	Male	Female
$\tau_{knee_f}$	60	39
$\tau_{knee_e}$	119	71
$\tau_{hip_f}$	105	70
$\tau_{hip_e}$	228	150

measurements were collected from a healthy subject pedaling with one leg on a planar surface.

Both plots feature a minimum around  $200^\circ$  and a maximum around  $270^\circ$ – $360^\circ$ . During regions of positive  $\tau_g$ , the simulated torque exceeds the measured torque because the user succumbs to gravity. When  $\tau_h$  is small, each joint torque is inefficiently converted, which impedes the onset of pedaling.

We discuss assistance methods for one-leg pedaling with the above characteristics. Assistance control for two-leg pedaling is generally implemented by multiplying the crank torque by a constant, as in power assisted bicycles. Our previous study demonstrated that pedaling with one leg placed undue load on the healthy leg. However, when the pedaling characteristics preclude easy application of the crank torque, simply multiplying the assisting torque by a constant may be insufficient to initialize pedaling.

Assist torque can be determined from the pedaling characteristics. If the pedal is in a difficult position, assistance is applied. Before supplying the assistance torque, the direction in which the user wants to travel must be known. Hence, we infer that the control must not only overcome the difficulty of pedaling but also must know the user-desired direction and magnitude of the assistance torque.

As discussed above, gravity contributes to the input pedaling torque. Thus gravitational effects must be removed from the crank torque. In the proposing control method, the operating torque  $\tau_h$  is assisted instead of net input torque  $\tau_{input}$ . In addition, the assistance ratio should not be constant because the conversion efficiency depends on the angular position of the pedal. Instead, we multiply the operating torque  $\tau_h$  by a varying assistance ratio derived in the next section.

## V. ASSISTING CONTROL METHOD FOR ONE-LEG PEDALING

This section introduces the proposed assistance control method for one-leg pedaling. The operating crank torque is assisted by a function of pedaling-assist-ratio. The operating crank torque is obtained by removing gravity effect of human leg from input crank torque. The gravity effect of human leg on crank torque is obtained by Eq.(6)-(9).

The conversion of the input torque was discussed in previous pedaling characteristics section. It showed how the joint torque is converted to crank torque, however, it was not enough because the constant joint torque had to be given. Thus, we consider potential joint torque range to find potential input torque.

Define torque ranges of leg joints  $\tau_{hip_f}$  as maximum flexor torque of hip,  $\tau_{hip_e}$  as maximum extensor torque of hip,  $\tau_{knee_f}$

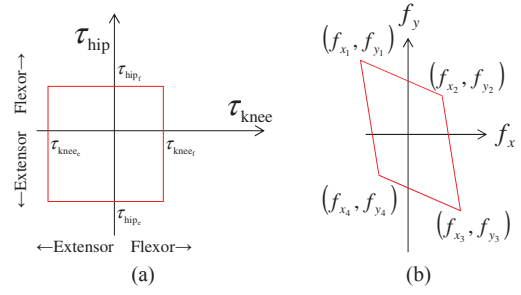


Fig. 7: Images of (a) Joint Torque Range and (b) Operating Force Range of Foot

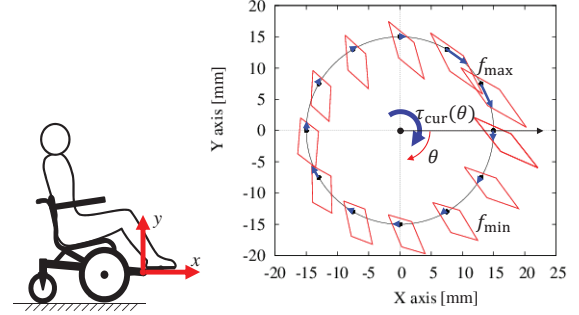


Fig. 8: Potential Pedaling Force around Pedaling Circle

as maximum flexor torque of knee and  $\tau_{knee_e}$  as maximum extensor torque of knee, as shown in Table I.

The joints are also affected by gravity on leg parts, such that when the joint is moving towards the gravity, the joint can exert as much more as the gravity effect of leg parts on the joint. The gravity effect on each joints differ due to the leg posture. The gravity effect on each joints are shown in Fig.5. The gravity effect on each joints are included in the potential joint torques.

Assuming that human can exert each maximum torques independently, the image of the torque range of the leg is shown in Fig.7(a). These torques are defined positive in flexor direction of each joints. The force range on pedal is calculated using virtual work principle,

$$\begin{bmatrix} f_{x1} & f_{x2} & f_{x3} & f_{x4} \\ f_{y1} & f_{y2} & f_{y3} & f_{y4} \end{bmatrix} = \left( \begin{bmatrix} \frac{\partial X_{foot}}{\partial \alpha} & \frac{\partial X_{foot}}{\partial \beta} \\ \frac{\partial Y_{foot}}{\partial \alpha} & \frac{\partial Y_{foot}}{\partial \beta} \end{bmatrix}^T \right)^{-1} \begin{bmatrix} \tau_{hip_f} & \tau_{hip_e} & \tau_{knee_f} & \tau_{knee_e} \end{bmatrix}, \quad (11)$$

where  $(X_{foot}, Y_{foot})$  is the position of the pedal from the position of the hip joint,  $(f_{x1}, f_{y1})$ ,  $(f_{x2}, f_{y2})$ ,  $(f_{x3}, f_{y3})$ , and  $(f_{x4}, f_{y4})$  are potential forces exerted by combinations of  $\tau_{hip_f}$ ,  $\tau_{hip_e}$ ,  $\tau_{knee_f}$ , and  $\tau_{knee_e}$ . The image of the force range is shown in Fig.7(b) which would be a parallelogram because it was transformed from rectangular-shaped torque range.

Figure 8 shows examples of potential operating force around pedaling circle. The parallelograms are angled from the circle. Especially when crank angle  $\theta$  is around  $65^\circ$  and  $240^\circ$ , the major axes of the parallelograms are nearly perpendicular to the circle. In this case it is difficult for the



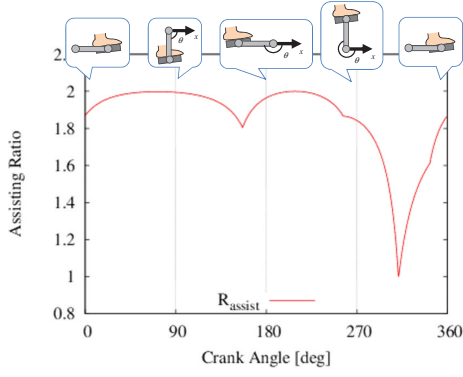


Fig. 9: Assist Ratio

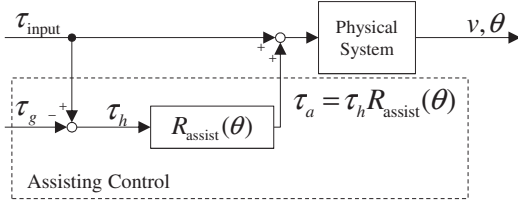


Fig. 10: Block Diagram of the Proposed Assisting Control

human leg to apply force in direction of crank torque. On the other hand, it is easier when  $\theta$  is around  $300^\circ$ .

Several conditions are required to be considered to obtain assist ratio function; (a) the ratio should be high when human joint torque is converted at low efficiency, (b) the ratio should be low when human joint torque is converted at high efficiency, and (c) the range of the ratio should be given considering rehabilitation use of the control. Thus, we define the assist ratio function  $R_{\text{assist}}(\theta)$  as follows;

$$R_{\text{assist}}(\theta) = R_{\min} + (R_{\max} - R_{\min}) \frac{\tau_{\max} - \tau_{\text{cur}}(\theta)}{\tau_{\max} - \tau_{\min}}, \quad (12)$$

where  $R_{\min}$  and  $R_{\max}$  are given range of the ratio function such that  $R_{\min} \leq R_{\text{assist}}(\theta) \leq R_{\max}$ .  $\tau_{\text{cur}}(\theta)$  is the potential crank torque of current position obtained by the potential operating force to exert the maximum crank torque, shown by the arrows in Fig.8,  $\tau_{\min}$  is the minimum of  $\tau_{\text{cur}}(\theta)$  and  $\tau_{\max}$  is the maximum of  $\tau_{\text{cur}}(\theta)$  in the pedaling cycle. For example, in Fig.8, the  $\tau_{\max}$  is the  $\tau_{\text{cur}}(\theta)$  of around  $\theta = 300^\circ$ . An example of the assistance ratio is graphed in Fig.9, when  $1 \leq R_{\text{assist}}(\theta) \leq 2$ .

The ratio shows minimum 1 when it is the easiest to apply crank torque for basic support. It increases as  $\tau_{\text{cur}}(\theta)$  decrease, so that the crank torque is more supported when  $\tau_{\text{cur}}(\theta)$  is small. The ratio around  $30^\circ$  shows maximum peak, because the ellipsoid is thinner than that of the opposite side.

Hence the assisting torque is obtained:

$$\tau_a = \tau_h R_{\text{assist}}(\theta) = (\tau_{\text{input}} - \tau_g) R_{\text{assist}}(\theta) \quad (13)$$

The control block diagram is shown in Fig.10.

## VI. EXPERIMENT OF THE ASSISTING CONTROL

In the experiment of the proposed assisting control, planar floor and uphill incline environment was used because the

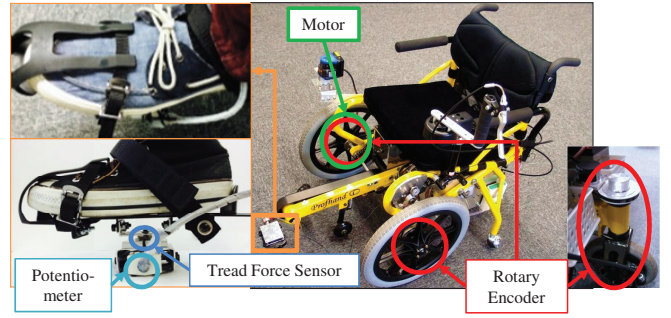


Fig. 11: System for Experiment

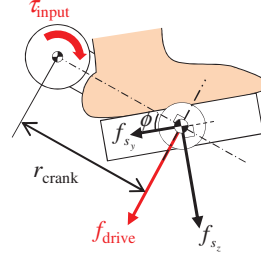


Fig. 12: Tread Force and Pedal Angle Detection

method is about assisting simple pedaling task. It was tested by four healthy subjects, pedaling with one leg.

The system is shown in Fig.11. A servo motor with rotary encoder is attached to the driving right wheel. Tread forces  $f_{sy}$  and  $f_{sx}$  are detected by 2 axes force sensor on the pedal. The input torque is obtained using the tread forces and the pedal angle  $\phi$  by the potentiometer attached to the pedal. Directions of detectable tread forces and angle are shown in Fig.12.

$$\tau_{\text{input}} = f_{\text{drive}} r_{\text{crank}} = (f_{sy} \sin \phi + f_{sx} \cos \phi) r_{\text{crank}} \quad (14)$$

Example results of one leg pedaling on planar floor are shown in Fig. 13. The result with conventional control provided large assist torque when input torque is large, on the other hand it is small when input torque is small. In contrast, result with proposed control provided large assist torque when input torque is small. The assisting torque is negative when  $\theta$  is  $0^\circ$ – $90^\circ$ , because the subject put a slight brake on to keep the velocity constant. In order to maintain condition of the experiment, the velocity was kept around the same. The smooth pedaling and controllability were also reported from the participants.

The mean work done by operating torque  $\tau_h$  per pedaling cycle on planar floor and uphill incline by all the subjects is shown in Fig.14. As it was shown in the results samples, the work is decreased in both environments.

## VII. CONCLUSION

This paper has presented and discussed the characteristics of one-leg pedaling of a cycling wheelchair. The pedaling motion involves human operating torque and gravity on leg. The simulated pedaling pattern closely corresponds to

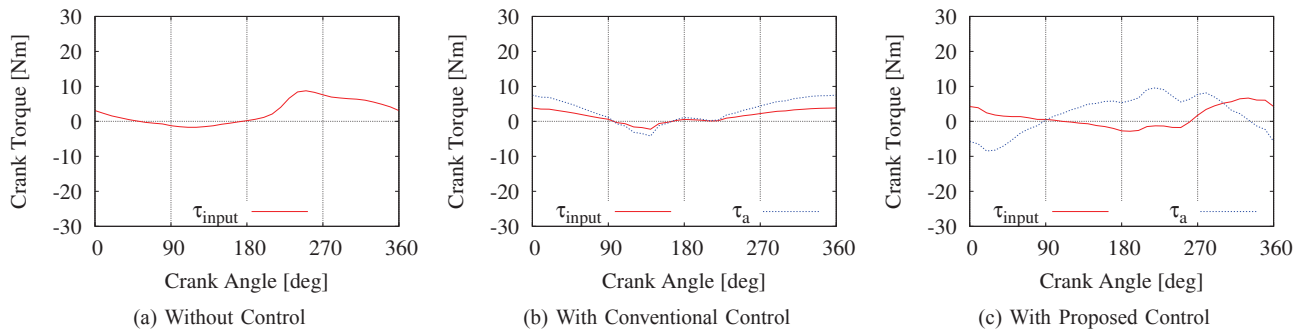


Fig. 13: Crank Torque on Planar Floor

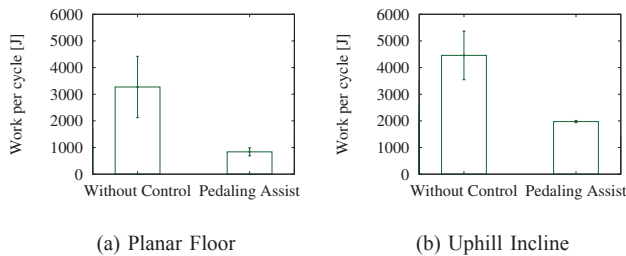


Fig. 14: Work per Pedaling Cycle of Operating Torque

the measured human pedaling pattern. From the observed characteristics, we proposed an assistance control method for one-leg pedaling. The human operating torque was multiplied by the assistance ratio derived from the maximum leg joint torques. The control method was validated in the experimental results. This study aimed to elucidate the basic characteristics of pedaling motion; therefore, the method was tested on four healthy subjects. In future, the method will be assessed by subjects with lower-limb disabilities.

## REFERENCES

- [1] T. Takahashi, Y. Nishiyama, Y. Ozawa, E. Nakano, and Y. Handa, "Cycling Chair: a novel vehicle for the lower limbs disabled," ICMIT 2005: Mechatronics, MEMS, and Smart Materials, Proceedings of SPIE, vol. 6040, p. 60401X, 2005.
- [2] K. Seki, M. Sato, T. Fujii, and Y. Handa, "Driving a cycling chair without FES in the non-ambulatory hemiplegic patients," Proceedings of 9th Annual Conference on International FES Society, 2004.
- [3] K. Seki, M. Sato, and Y. Handa, "Increase of Muscle Activities in Hemiplegic Lower Extremity During Driving a Cycling Wheelchair," The Tohoku journal of experimental medicine, vol.219, no.2, pp.129-138, 2009.
- [4] A. Kaisumi, Y. Hirata, K. Kosuge, "Investigation of User Load and Evaluation of Power Assistive Control on Cycling Wheelchair," Journal of Robotics and Mechatronics, vol. 25, no. 6, pp. 959-965, 2013.
- [5] Y. Hirata, K. Kawamata, K. Sasaki, A. Kaisumi, K. Kosuge, E. Monacelli, "Regenerative brake control of cycling wheelchair with passive behavior," IEEE International Conference on Robotics and Automation, pp. 3873 - 3879, 2013.
- [6] N. Hiro, E. Takeuchi, K. Ohno and S. Tadokoro, "Developing a measurement system for improving daily lives of Cycling Wheel Chair patients," Proceedings of SICE Annual Conference, pp.1656-1660, 2012.
- [7] N. Sugita, Y. Kojima, M. Yoshizawa, A. Tanaka, M. Abe, N. Homma, K. Seki and N. Handa, "Development of a virtual reality system to evaluate skills needed to drive a cycling wheel-chair," IEEE Annual International Conference of Engineering in Medicine and Biology Society, pp. 6019-6022, 2012.
- [8] N. Sugita, M. Yoshizawa, Y. Kojima, A. Tanaka, M. Abe, N. Homma, T. Kikuchi, K. Seki and Y. Handa, "Evaluation of navigation skill of elderly people using the cycling wheel chair in a virtual environment," IEEE Virtual Reality 2013, pp.125-126, 2013.
- [9] L. Schutte, M. Rodgers, F. Zajac and R. Glaser, "Improving the Efficacy of Electrical Stimulation-Induced Leg Cycle Ergometry: An Analysis Based on a Dynamic Musculoskeletal Model," IEEE Transactions on Rehabilitation Engineering, vol. 1, no. 2, pp. 109-125, 1993.
- [10] M. Gföhler and P. Lugner, "Cycling by Means of Functional Electrical Stimulation," IEEE Transactions on Rehabilitation Engineering, vol. 8, no. 2, pp. 233-243, 2000.
- [11] M. Gföhler, T. Angeli, T. Eberharter, P. Lunger, W. Mayr and C. Hofer, "Test Bed with Force-Measuring Crank for Static and Dynamic Investigations on Cycling by Means of Functional Electrical Stimulation," IEEE Transactions on Neural Systems and Rehabilitation Engineering, vol. 9, no. 2, pp. 169-180, 2001.
- [12] J. Rosecrance and C. Giuliani, "Kinematic Analysis of Lower-Limb Movement During Ergometer Pedaling in Hemiplegic and Nonhemiplegic Subjects," Physical Therapy, vol.71, no.4, pp.334-343, 1991.
- [13] D. Brown, S. Kautz and C. Dairaghi, "Muscle Activity Adapts to Anti-gravity Posture during Pedaling in Persons with Post-stroke Hemiplegia," Brain, vol.120, pp.825-837, 1997.
- [14] D. Brown and S. Kautz, "Increased Workload Enhances Force Output During Pedalling Exercise in Persons With Poststroke Hemiplegia," Stroke, vol.29, pp.598-606, 1998.
- [15] H. Saitou, H. Yanagi, S. Hara, S. Tsuchiya, S. Tomura, "Cerebral Blood Volume and Oxygenation Among Poststroke Hemiplegic Patients: Effects of 13 Rehabilitation Tasks Measured by Near-Infrared Spectroscopy," Archives of Physical Medicine and Rehabilitation, vol. 81, pp.1348-1356, 2001.
- [16] Y. Nakanishi, I. Mizuuchi, T. Yoshikai, T. Inamura and M. Inaba, "Pedaling by a Redundant Musculo-Skeletal Humanoid Robot," Proceedings of 2005 5th IEEE RAS International Conference on Humanoid Robots, pp. 68-73, 2005.
- [17] K. Kosuge, H. Yabushita and Y. Hirata, "Load-free Control of Power-Assisted Cycle," TExCRA '04 First IEEE Technical Exhibition Based Conference on Robotics and Automation, pp. 111-112, 2004.
- [18] I. Pontaga, "Hip and knee flexors and extensors balance in dependence on the velocity of movements," Biology of Sport, vol. 21, no. 3, pp. 261-272, 2004.
- [19] Dinesh Samuel and Philip J. Rowe, "Effect of Ageing on Isometric Strength through Joint Range at Knee and Hip Joints in Three Age Groups of Older Adults," Gerontology, vol. 55, no. 6, pp. 621-629, 2009.
- [20] Paulo Cesar Barause Bento, Gleber Pereira, Carlos Ugrinowitsch and Andre Luiz Felix Rodacki, "Peak torque and rate of torque development in elderly with and without fall history," Clinical Biomechanics, vol. 25, pp. 450-454, 2010.